ELSEVIER

Polymer 41 (2000) 5315–5326

polymer

Blends of bitumen with various polyolefins

A.H. Fawcett*, T. McNally[1]

School of Chemistry, The Queen's University of Belfast, Stranmillis Rd, Belfast BT9 5AH, Northern Ireland, UK

Received 21 July 1999; received in revised form 15 September 1999; accepted 29 September 1999

Abstract

Blends of a 100 penetration grade bitumen have been prepared at 180°C with five different polyolefins, each in four different proportions (10, 20, 30 and 40 pph). They have been examined by fluorescence microscopy at ambient temperatures, and by DSC and DMTA over a wide temperature range. DSC indicated that the melting points of crystallites formed on cooling the blends were about 10°C lower than for the pure polymer, for the crystallites were smaller in size. The stiffness of the bitumen was enhanced at low temperatures by 100 fold and at high temperatures to an even greater extent by the polymers, the sole exception being blends of an atactic polypropylene, whose moduli at low temperatures were the same as the bitumen. Loss processes were seen with all the polymers, the temperature falling from about 55°C for the isotactic polypropylene blends to about −30°C for the ethylene–propylene rubber. Their Arrhenius activation energies fell from 1300 to about 160 kJ mol^{-1} with temperature and as the crystallinity fell in the blend. The 40 pph blend of the isotactic polymer may have extensive lamellar morphology, for it was as stiff at 150°C as the bitumen at −20°C. Several of the other polymers formed an amorphous and extensive polymer-rich phase. In general, the blends lost modulus suddenly when the temperature rose above the melting points of the crystallites, which, until then, served to crosslink the polymer to form a gel.

Keywords: Bitumen; Polyolefins; Blends

1. Introduction

In this paper we examine the properties of blends of a bitumen with a number of polyolefins, as an extension of our studies on four polyethylenes [1]. Such blends may have applications in built-up roofing membranes [2] and in other waterproofing uses. Further uses may follow from a study of the materials that establishes their properties and leads to an understanding of their performance. As Table 1 records, two propylene homopolymers were used, one a completely isotactic polymer, the other an atactic polymer. The former sample from Exxon Chemicals was a semi-crystalline polymer, the latter sample a commercially available material (MF5) from Dussek–Campbell APP Polymers which is nominally atactic polypropylene (APP), and is regularly blended with bitumen for roof making membranes [2]. It was obtained as a by-product from early plants that manufactured isotactic polypropylene (IPP), for the catalyst (used in the production process) contained a small fraction of active sites, which yielded the atactic polymer and also some low molecular weight species. The similar low molecular weight by-product of ethylene–propylene (EP) copolymer is also present. MF5 also contains a proportion (<5%) of the isotactic polymer which probably derives from the original polymerisation, and is produced free of polymerisation solvent in the form of liquids to soft solids.

Three commercial copolymers of ethylene and propylene were also blended with bitumen; the first was a block copolymer, Adflex, from Himont (now Montell Polyolefins), where the propylene blocks are grafted onto the main chain ethylene blocks. The exact nature of the blocks of such copolymers is not satisfactorily understood and is a subject of considerable interest. Prasad [3] has used solid state ^{13}C NMR spectroscopy with cross polarised magic angle spinning and high power dipolar coupling to characterise the 'block' structure of Adflex copolymers. A signal due to block junctions appears in the spectra of block copolymers only at 32.5δ which is absent in random copolymers. The second copolymer used was an EP rubber from Exxon Chemicals with 40% by weight of ethylene residues. The monomers are in a random distribution along the polymer chain and sequences of homopolymer are short. The final copolymer used, Vestoplast 891, was one of a series of predominately amorphous polyolefins from Hüls which have been specifically developed for bitumen modification. They may be manufactured by the

* Corresponding author. Tel.: +44-0-1232-274-405; fax: +44-0-1232-382-117.

[1] Present Address: MVC Technology Research Group, Polymer Research Centre, The Queen's University of Belfast, Belfast BT9 5AH, UK.

0032-3861/00/$ - see front matter
PII: S0032-3861(99)00733-8

Table 1
The polymers used in this study

Polyolefin	Source	Grade
IPP	Exxon Chemicals	Escorene PP 3684FI
APP	Dussek–Campbell Ltd—APP Polymers Division	MF5
α-olefin copolymer	Hüls	Vestoplast 891
EP graft copolymer	Himont	Adflex 7084 F XCP
EP rubber	Exxon Chemicals	Vistalon 404

low pressure copolymerisation of α-polyolefins (ethylene, propylene and isobutylene) [4] utilising heterogeneous catalysts and have a low crystalline content. Polymers made using heterogeneous catalysts often exhibit compositional heterogeneity arising from multiple catalytic sites [5,6]. A series of multiple structures is formed, comprising blocky and random copolymers and homopolymers of ethylene and propylene. The catalysts used yield a random structure, which interferes with the crystallisation processes, so a predominately amorphous polymer is obtained. These

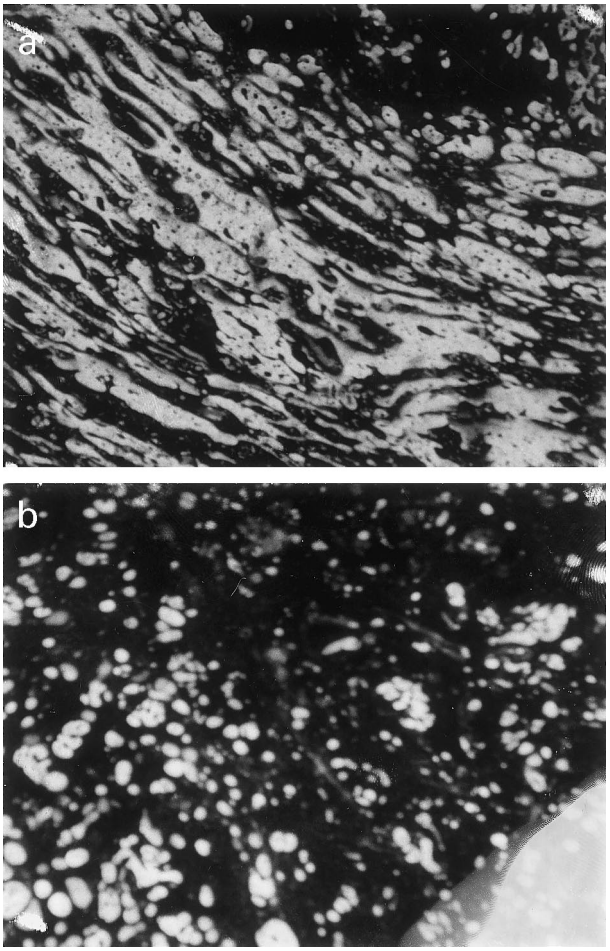

Fig. 1. Fluorescence photomicrographs of blends of 30 and 40 pph IPP with 100 pen. bitumen (105×).

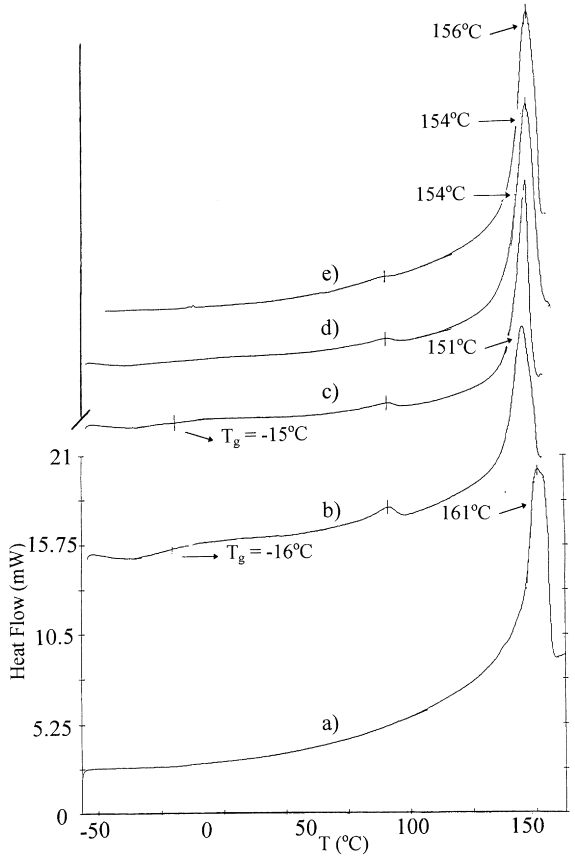

Fig. 2. DSC curves of: (a) IPP; (b) 10 pph; (c) 20 pph; (d) 30 pph; and (e) 40 pph blends of IPP with pen. bitumen.

results may be relevant to the modification of bitumen for improving its properties in roofing [2], and road paving [7–9] applications.

The bitumen, of a Venezuelan 100 penetration grade (100 pen.) provided by Nynas and often used in commercial blends of MF5, had an aromatic:paraffin:resin:asphaltene proportion of 47:6:16:31, as determined by Iatroscan analysis [1], and is thus itself a complicated colloidal material even before any polymeric material is added [8]. Since all the polymers have the elemental formula $(CH_2)_x$, their intermolecular forces correspond most closely to the paraffin component. The concentrations we employ (9, 16, 23 and 28%) approach the region at which chain entanglements become possible, and the range of temperatures takes the materials from stiff solids to fluids [10].

2. Experimental

Blends were prepared at high temperatures in a Z-blade mixer with 10, 20, 30 and 40 pph polymer, and samples were examined by fluorescence microscopy, DSC and DMTA as has been described previously [1]. The bitumen was studied in the shear mode (DMTA) in this journal as it became soft on warming.

Table 2
DSC characteristics of blends of bitumen with, IPP

pph Polymer	10	20	30	40	IPP
% Polymer	9.1	16.7	23.1	28.6	100
T_g of blend (°C)	−22	−20	−18	−14	−20[a]
T_m of blend (°C)	151	154	154	156	161
$\Delta C_p T_g$ process (J g^{-1} deg^{-1})	0.07	0.04	very small	very small	NA[b]
ΔHT_m process (J g^{-1})	7.30	14.75	19.46	26.80	84.34
ΔHT_m process calculated[c]	7.67	14.08	19.48	24.10	NA[b]

[a] Literature value pure polymer [13].
[b] Not applicable.
[c] Calculated from 84.34 × % polymer/100.

3. Results and discussion

3.1. Isotactic polypropylene

The fluorescence photomicrographs of these blends display two phases, whatever the proportion of the polymer, as may be seen in Fig. 1 for the 30 and 40 pph blends. The proportion of the light toned polymer-rich phase increased with increasing polymer proportion, but it did not become continuous. The IPP alone displayed just one process in its DSC trace (see Fig. 2), an endotherm with a maximum at 161°C and extending upwards from about 110–165°C, the range of melting associated with the crystallites of IPP having different sizes [11,12]. The blends revealed two main features in their DSC traces, a glass transition process with a T_g at −22°C for the 10 pph blend rising to −14°C for the blend consisting of 40 pph IPP. The step height for this low temperature process was small for all the blends and decreased with increasing IPP concentration in the blend, and thus was associated with the bitumen-rich dispersed medium. The second main feature was an endotherm having a peak maximum at 151°C for the 10 pph blend rising slightly to 156°C for the 40 pph blend with bitumen and was about 5–10°C below the T_m we obtained for the IPP itself. The presence of the bitumen has apparently disrupted the IPP crystallites yielding smaller less perfect crystallites which in turn have lower melting temperatures [11–13]. Commercial samples routinely melt between 160 and 165°C, much below the thermodynamic melting point of 188°C [14]. A third minor feature was seen at about 86°C in all the blends, it became less intense with increasing IPP concentration. According to the DSC values of enthalpy of

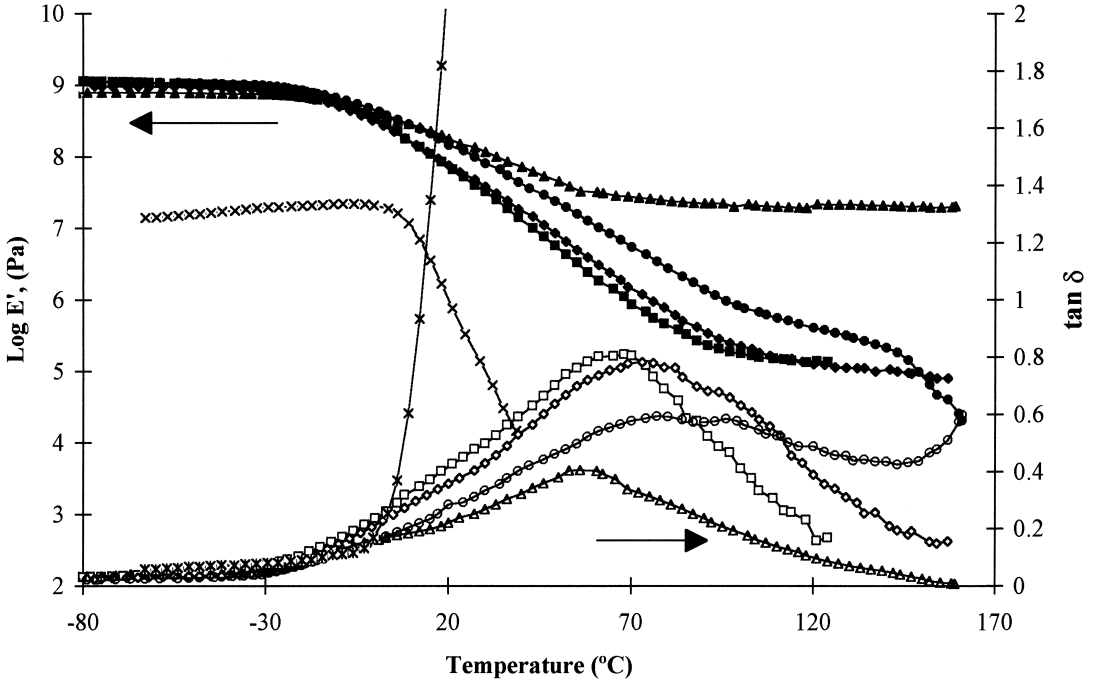

Fig. 3. Variation in storage modulus E' (stiffness) and tan δ with composition for blends of IPP with 100 pen. bitumen, from DMTA studies at 1 Hz. The blends are distinguished as follows: 10 pph, squares; 20 pph, diamonds; 30 pph, circles; 40 pph, triangles; filled symbols, E'; open symbols, tan δ; the bitumen itself, crosses. The value of E' for the bitumen has been adjusted by a factor of 3, since it was measured in the shear mode [15].

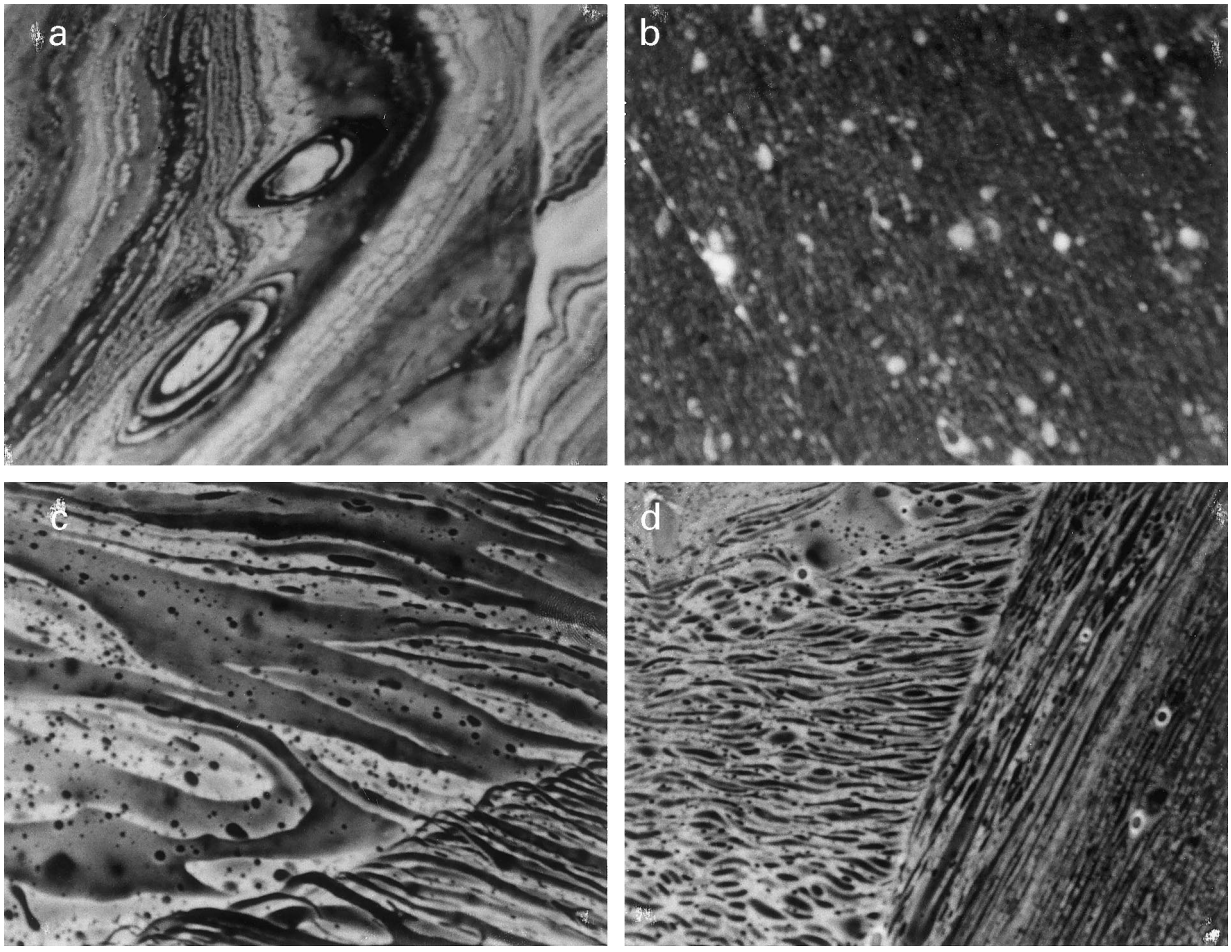

Fig. 4. Fluorescence photomicrographs of blends of: (a) 10 pph; (b) 20 pph; (c) 30 pph; and (d) 40 pph APP (MF5) with 100 pen. bitumen, (105×).

melting of the main peak, to within 5% the enthalpy value (ΔH) for the first blend is just that value which would be obtained if all the IPP was present only in a crystalline phase, Table 2. For the final (40 pph) blend, the ΔH melting is higher than predicted from the composition, so there is little evidence for the polymer dissolving in the bitumen to produce a modified amorphous phase. This contrasts with the behaviour of the polyethylenes [1], whose crystalline components were reduced in proportion by the bitumen.

The tan δ and storage modulus versus temperature plots are shown in Fig. 3 for the IPP blends. The tan δ curves display one main process with peak maxima at about 60°C for each of the blends, the intensity of each peak decreasing with increasing IPP content. A shoulder to this peak develops at about 0°C as the polymer content rises, a contribution from an amorphous polypropylene phase. It may be seen from the storage modulus (E') traces below −10°C that the blends are about two orders of magnitude stiffer than bitumen itself. However, all the blends begin to soften below the temperature at which bitumen itself softens, this property of the blends being derived from their DSC-determined glass transition temperature (T_gs) lying between −14 and −22°C (see Fig. 2). The storage modulus curves of the 10, 20 and 30 pph blends reached a plateau at approximately 100°C, and at 60°C for the 40 pph blend. These plateaux terminated between 155 and 160°C when the samples began to flow within the bending mode measurement system (and we ceased heating). These softening temperatures are similar to the T_m of the blends obtained by DSC. This pattern of behaviour is consistent with the crystallite network or gel structure which disperses when the crystallites melt, as we found for a polyethylene sample in this bitumen [1], and as has been described for several polymer–solvent systems [13]. Notice that at 150°C the 40 pph blend has a modulus about 200 times that of the 10 and 20 pph blends, that it is only about 50 times less at −50°C, and that at 150°C the blend is a little stiffer than the bitumen alone at −50°C. This suggests the presence in the 40 pph blend of an extensive, even percolating, crystalline structure. The fact that only the high (40 pph) IPP content blend has a modulus extending to the higher melting point of the crystallites indicates that there may be two types of crystallites: studies of polyethylene–solvent gels suggested fringed micelles extended chain crystals as well as lamellae from folded chains [12]. The latter may form also in this system when the IPP content is high.

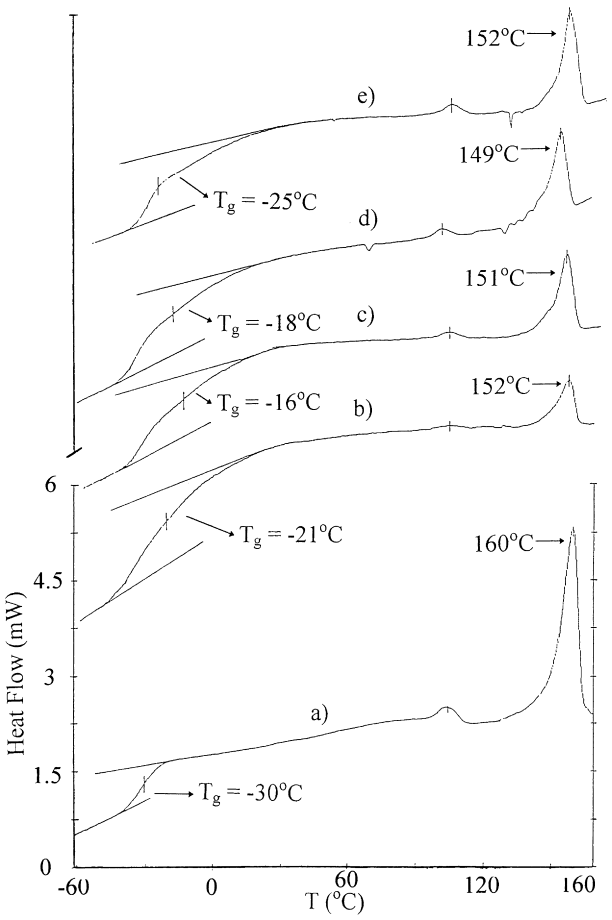

Fig. 5. DSC curves for: (a) APP (MF5); (b) 10 pph; (c) 20 pph; (d) 30 pph; and (e) 40 pph blends of MF5 with 100 pen. bitumen.

3.2. Atactic poly(propylene): MF5

This material, nominally APP, has been found by inspection of its ^{13}C NMR spectrum to contain proportions of EP copolymer of low molecular weight [4] as well as some IPP. MF5 blended easily with 100 pen. bitumen at all compositions. The fluorescence photomicrographs exhibited two phases, a light coloured polymer-rich phase and a dark area we associate with the bitumen-rich phase, see Fig. 4. For the 10 and 20 pph blends the polymer-rich phase is limited in extent, but it appears to extend over all the area for the 30 and 40 pph blends, a feature termed "phase inversion" [2]. As the latter blends contain only 23 and 28% of polymer, respectively and yet the polymer-rich phase covered more than half the area of the photomicrograph, the polymer-rich phase must contain some components of the bitumen such as paraffins and aromatics, the latter probably being responsible for the fluorescence. Phase inversion occurred at a loading of MF5 in the blends between 20 pph (16% (w/w)) and 30 pph (23% (w/w)) according to the photomicrographs and is routinely sought when making blends for built-up roofing membranes. Large striations in the 30 and 40 pph blends were also observed, with spacing of the order of 10–50 μm, from the manner in which the mixing process had distorted the shape of the phases.

The DSC traces for the polymer and its blends displayed endothermic peaks that extended upwards from about 130°C, the peak maxima for the blends being some 8–11°C below that of the pure polymer (Fig. 5). This higher temperature transition is not associated with the atactic polymer but rather with IPP, which has been carried over

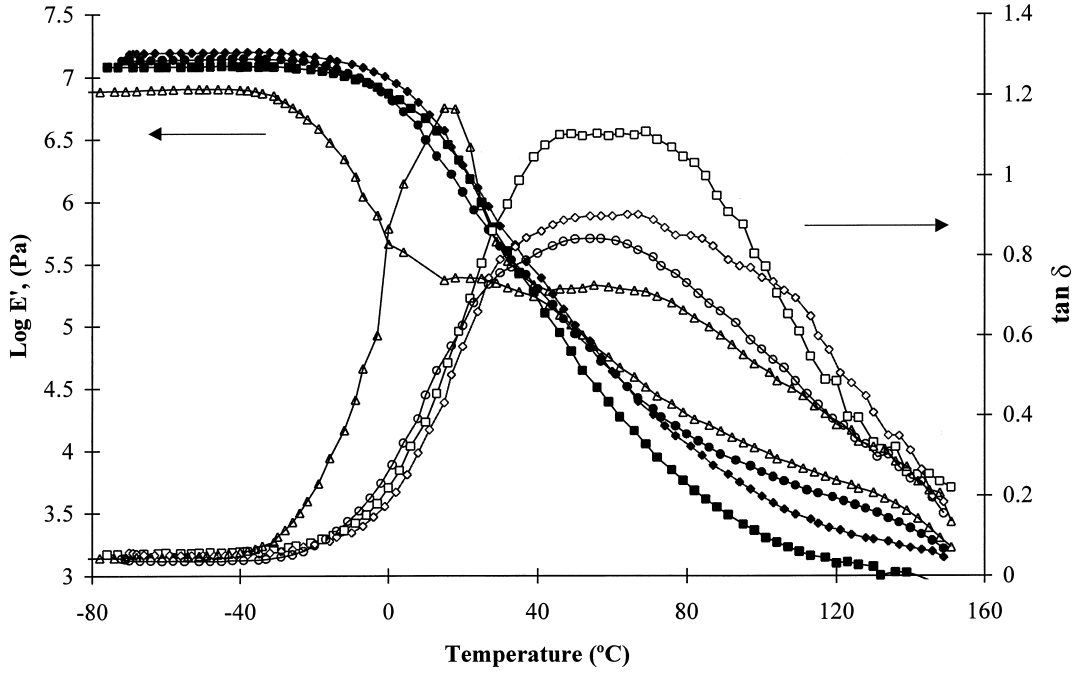

Fig. 6. Variation in storage modulus E' (stiffness) and tan δ with composition for blends of APP (MF5) with 100 pen. bitumen, from DMTA studies at 1 Hz. The blends are distinguished as follows: 10 pph, squares; 20 pph, diamonds; 30 pph, circles; 40 pph, triangles; filled symbols, E'; open symbols, tan δ.

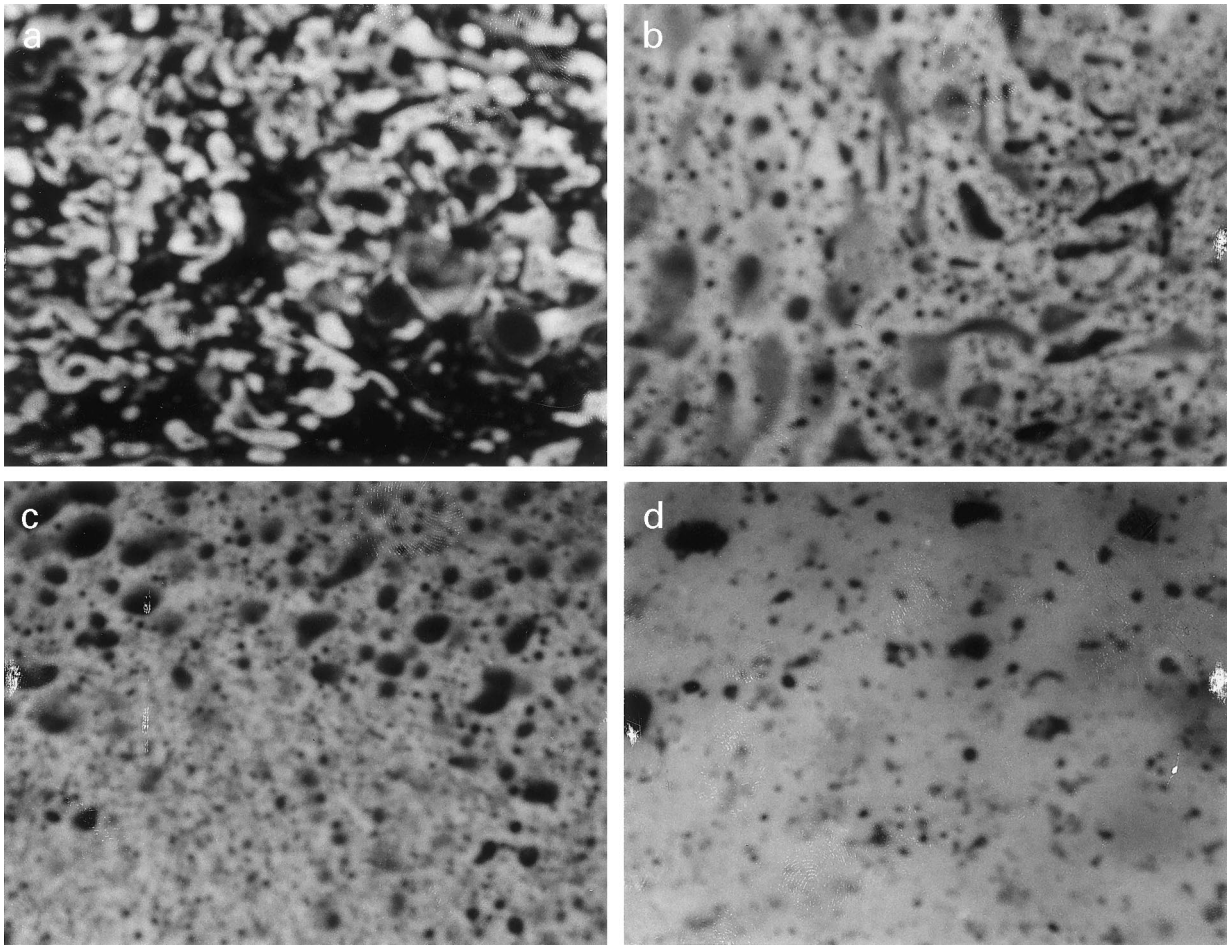

Fig. 7. Fluorescence photomicrographs of blends of: (a) 10 pph; (b) 20 pph; (c) 30 pph; and (d) 40 pph α-olefin copolymer (Vestoplast 891) with 100 pen. bitumen, (105×).

from the production process and from any semicrystalline polymer that may have been added to the atactic polymer. The depression of the polymer melting point by the presence of the bitumen may be attributed to the bitumen disrupting the crystalline component of the polymer, thus yielding crystallites with a distribution of smaller sizes, the critical dimension probably being thickness, as has been discussed for other polyolefins [11–13]. A second minor melting endotherm is also observed at about 105°C for both the polymer and the blends. This process occurs at roughly the melting temperature of crystallites of low-density polyethylene (LDPE) in its blends with 100 pen. bitumen [1], and so may originate from a small proportion of LDPE. MF5 itself has a T_g at approximately −30°C, and its blend's T_g was some 10°C higher. Close examination of the DSC traces obtained for the 30 and 40 pph blends reveals the possible presence of two T_gs. The lower temperature process we assume is derived from a polymer-rich phase, and the transition at about 0°C from a bitumen-rich phase, which is stiffened by asphaltenes.

Fig. 6 shows the variation of tan δ and storage modulus (E') with composition of the blends in the temperature range −120 to 150°C, respectively. All four blends persisted within the measurement system up to 150°C, but then the sample became too soft, making measurements impossible. It is probable that the crystallites of the IPP component we consider to be present were capable of producing a network by crosslinking the polymer chains until they melted at 150°C. The temperature at which the blends begin to flow is similar to the T_m values obtained from our DSC studies. Corresponding behaviour was also evident when the blends of 100 pen. bitumen with IPP only were examined, see Fig. 3 (where the E' for the bitumen is included), but the APP blends are softer by two orders of magnitude than the IPP blends at 150°C. The addition of small amounts of MF5 causes the modulus of the blends at −20°C to fall slightly below that of bitumen itself, the effect being most noticeable for the blend with 40 pph polymer for which phase inversion had produced an extensive polymer-rich phase. The tan δ curves for the 10, 20 and 30 pph blends displayed one broad loss process centred on 50 to 60°C whose intensity fell as the polymer content rose, whereas the 40 pph blend shows an extra large spike in tan δ at 10°C which we attribute to a large loss process in the polymer-rich phase. This process, for which there is little evidence in the low polymer concentration blends, starts as low as −30°C, reflecting the

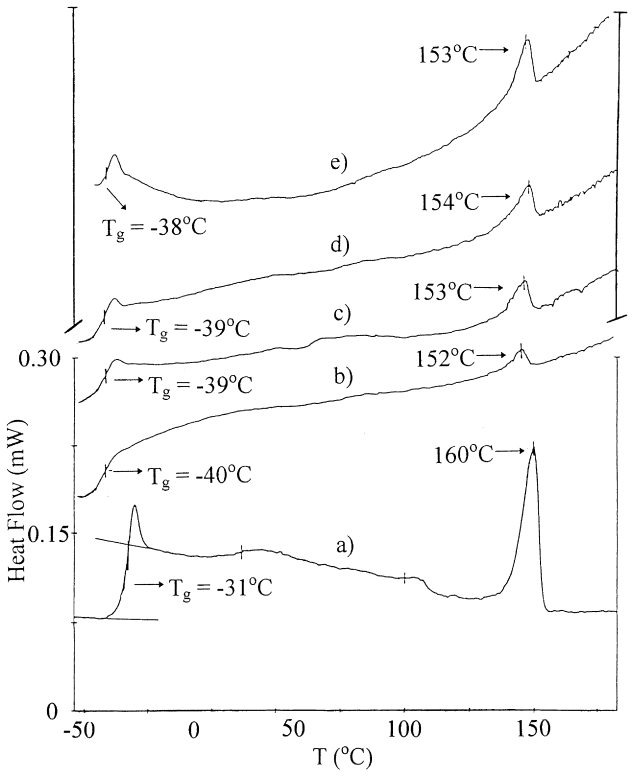

Fig. 8. DSC traces for: (a) α-olefin copolymer (Vestoplast 891); (b) 10 pph; (c) 20 pph; (d) 30 pph; and (e) 40 pph blends of Vestoplast 891 with 100 pen. bitumen.

flexibility induced by the APP in the 40 pph blend and which is required by a roofing system to prevent it cracking in cold environments. From this DMTA evidence, it is very clear that phase inversion, producing an extensive phase with a low T_g, took place above the 30 pph loading. The APP material may promote the formation of fringed micelle crystallites when the IPP content is <5%.

3.3. α-olefin copolymer: Vestoplast 891

The fluorescence photomicrographs of this polymer's blends with 100 pen. bitumen are shown in Fig. 7. The polymer-rich phase was continuous once the polymer concentration in the blend had reached the 20 pph level, the light coloured polymer-rich phase extending over a greater area with increasing polymer content in the blends. Phase inversion therefore takes place at some polymer loading below 20 pph (16% (^{w}/w)).

The polymer and its blends exhibit two main transitions in the DSC curves, see Fig. 8. The first is a glass transition at −31°C for the polymer, a process which (in contrast to the previous system) is depressed by some 7–9°C in the blends. The second feature is an endotherm at 160°C for the polymer and between 152 and 154°C for the blends, the enthalpy values for this process increasing with increasing polymer content, as recorded in Table 4. For Vestoplast 891 the main T_g process at −31°C and a minor transition at about 20°C may be attributed to the elastic copolymer structures. The main endothermic feature at 160°C and minor endotherm at about 100°C may be derived from crystallisable propylene and ethylene sequences within the random structures. The presence of the melting endotherm signifies the melting of polymer crystallites in the blends at these temperatures, similar to that seen for blends of MF5 with 100 pen. bitumen.

The variation in tan δ and storage modulus with composition is shown in Fig. 9. The blends persisted within the measurement system to 100, 115, 130 and 130°C for the blends containing 10, 20, 30 and 40 pph Vestoplast 891,

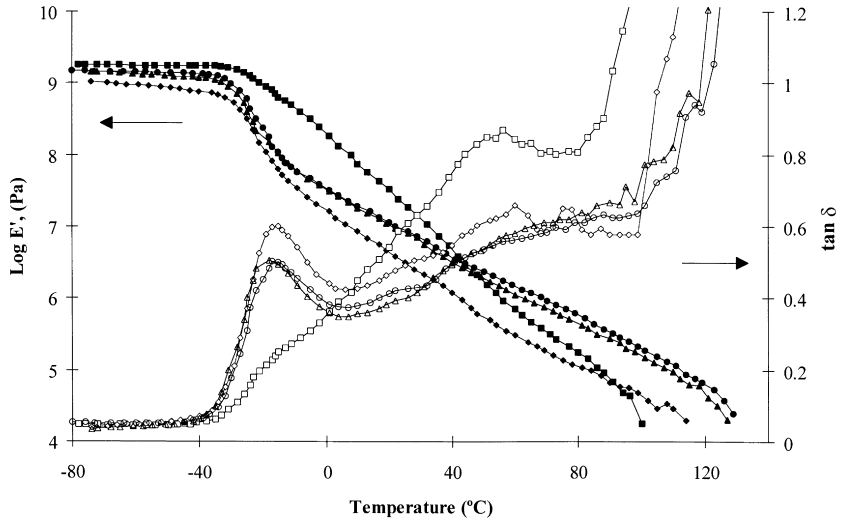

Fig. 9. Variation in storage modulus E' (stiffness) and tan δ with composition for blends of α-olefin copolymer (Vestoplast 891) with 100 pen. bitumen, from DMTA studies at 1 Hz. The blends are distinguished as follows: 10 pph, squares; 20 pph, diamonds, 30 pph, circles; 40 pph, triangles; filled symbols E'; open symbols, tan δ.

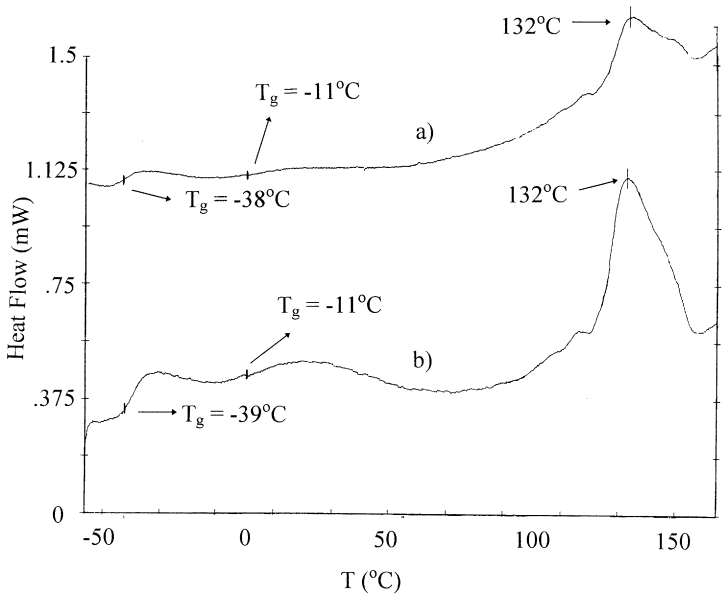

Fig. 10. DSC traces are: (a) 30 pph; and (b) 40 pph blends of EP graft copolymer (Adflex) with 100 pen. bitumen.

respectively. These values are between 20 and 50°C below the temperature at which the respective melting endotherms of the blends in the DSC curves were observed. The crystallite-crosslinked network model does not seem to apply to these blends. The tan δ plots show a clearly resolved low temperature loss process having a peak maximum at −17°C and extending upwards from −40°C for the 20, 30 and 40 pph blends. This observation is consistent with that seen in the loss modulus (E'') plots, the peak maxima for the 20, 30 and 40 pph blends being about 40°C lower than that of the bitumen itself. A maximum in tan δ for the 10 pph blend at 50°C diminished as the polymer content rose. All the blends are about two orders of magnitude stiffer than bitumen below −30°C; however, between −15 and 15°C the blends with 20, 30 and 40 pph Vestoplast are less stiff than bitumen itself, suggesting that an extensive polymer-rich phase develops at some point above 10 pph loading, an idea also supported by the good resolution of the tan δ peaks. Above 15°C all the blends are stiffer than bitumen alone, a property attributed to the presence of the viscous high molecular weight component.

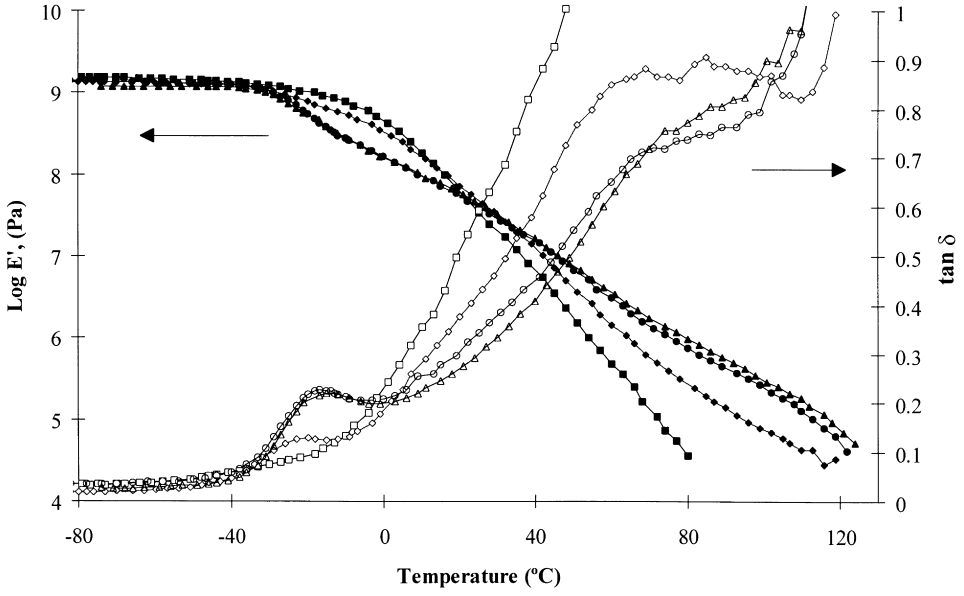

Fig. 11. Variation in storage modulus E' (stiffness) and tan δ with composition for blends of EP graft copolymer (Adflex) with 100 pen. bitumen, from DMTA studies at 1 Hz. The blends are distinguished as follows: 10 pph, squares; 20 pph, diamonds; 30 pph, circles; 40 pph, triangles; filled symbols, E', open symbols, tan δ.

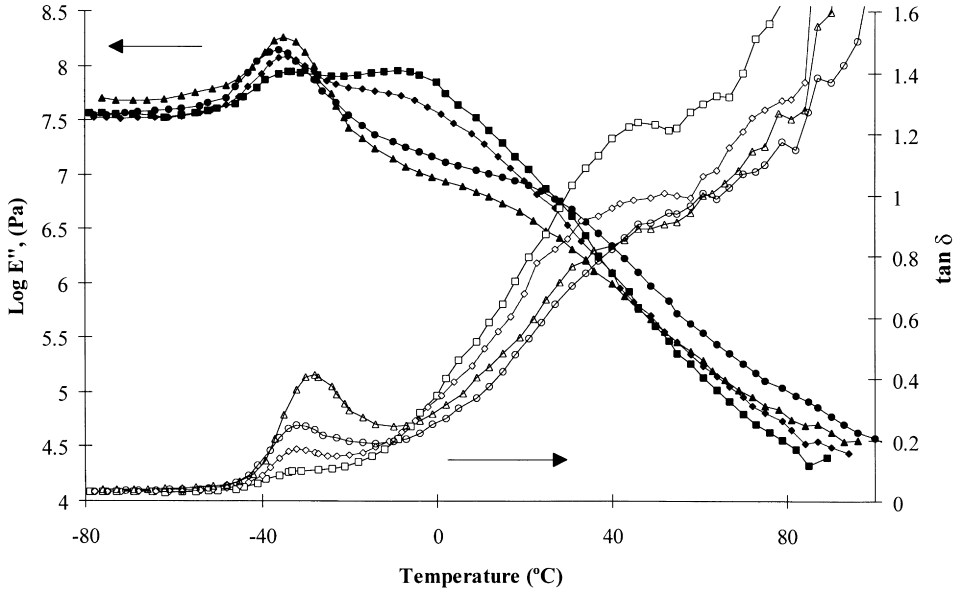

Fig. 12. Variation in loss modulus E'' and tan δ with composition for blends of EP rubber with 100 pen. bitumen, from DMTA studies at 1 Hz. The blends are distinguished as follows: 10 pph, squares; 20 pph, diamonds; 30 pph, circles; 40 pph, triangles; filled symbols, E'; open symbols, tan δ.

3.4. Ethylene–propylene graft copolymer: Adflex

The blends of this polymer with bitumen suggested, under fluorescence microscopy, the presence of two phases [16]. The polymer-rich phase was more dispersed into smaller regions, the higher the proportion of polymer. The remnants of streaks caused by the mixing have separated partially into droplets. It is not clear that an extensive phase is present from the photomicrographs, except for the 10 pph blend, which clearly shows droplets having diameters between 2 and 5 μm and coarser particles up to 10 μm in diameter of the polymer-rich phase dispersed in a bitumen-rich phase.

The DSC traces for each blend show three features, two glass transitions and one melting transition. Typical traces for the 30 and 40 pph blends are shown in Fig. 10. The melting endotherm shifts slightly upwards as the proportion of polymer in the blend is increased. The glass transition temperature values behave differently for the two features, the lower one staying at about −40°C whatever the composition of the blend, but growing in step size, and so coming from the polymer-rich phase. Confirmation of this is the

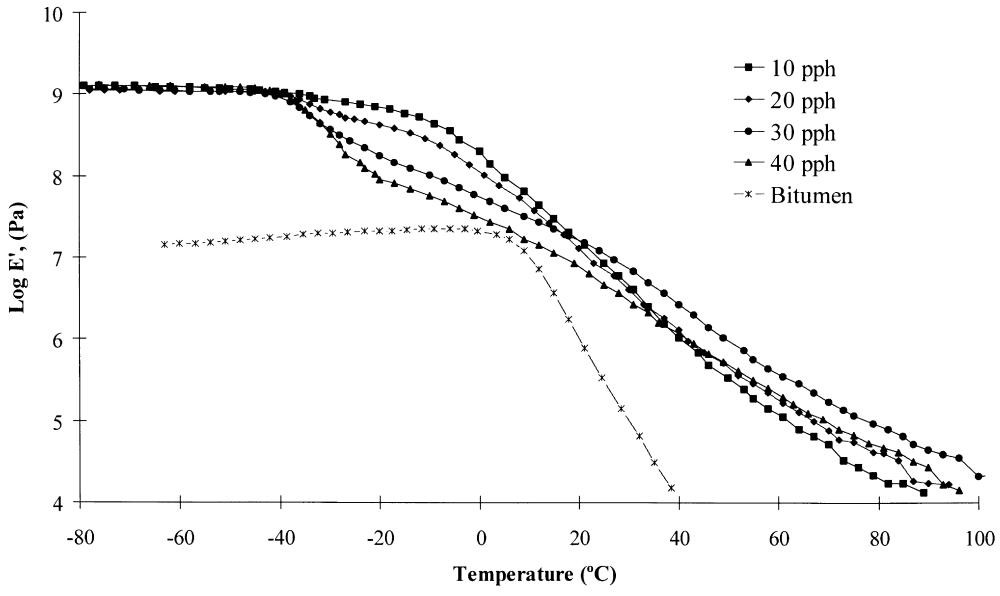

Fig. 13. Variation in storage modulus E' with composition for blends of EP rubber with 100 pen. bitumen measured at 1 Hz as a function of temperature, from DMTA studies.

Table 3
DSC characteristics of blends of bitumen with APP, MF5

pph Polymer	10	20	30	40	MF5
% Polymer	9.1	16.7	23.1	28.6	100
T_g (°C)	−21	−16	−35 & 2	−32 & 0	−30
T_m (°C)	152	151	149	152	160
ΔC_pT_g process (J g^{-1} deg^{-1})	0.24	0.23	0.21	0.23	0.26
ΔHT_m process (J g^{-1})	1.06	1.50	1.96	2.69	12.97

observation of the T_g at −37°C in the pure polymer. The other weaker transition was seen at a temperature that moved upwards from about −11 to 6°C, a movement that is presumed to be caused by an increasing proportion of the asphaltenes remaining in the bitumen-rich phase as the more flexible components are drawn to the polymer-rich phase.

The DMTA traces are shown in Fig. 11, the blend of lowest polymer proportion, 10 pph, being clearly insufficiently stiff to persist in the measurement system up to the melting point of the crystallites at 132°C. This is consistent with the bitumen-rich phase being extensive. Conversely, the other three blends were stiff enough to permit measurements up to the DSC observed melting region at about 130°C, which suggests that the polymer-rich phase is then extensive and a fringed micelle type of gel network might again exist. The three higher polymer content blends also showed a loss process at about −25°C (E'') and at −20°C (tan δ) at a frequency of 1 Hz, the feature being fully developed and at a slightly higher temperature in the traces of the 30 and 40 pph blends. The two lower polymer content blends show a loss process at about 0°C in the loss modulus (E'') traces. These loss processes were consistent with the observation of the presence of two glass transitions in the DSC curves.

3.5. Ethylene–propylene rubber: Vistalon

The fluorescence photomicrographs of the 10, 20 and 30 pph blends with 100 pen. bitumen displayed no discernible features [16], and so are not shown here, the rubber having only been melted, sheared and stretched during the mixing process. For the 40 pph blend the polymer-rich phase may extend over an area approximately equivalent to the 29% polymer present in the blend.

The EP rubber displayed three features in its DSC trace. The first, a glass transition process at −40°C and two small endotherms, one broad with a peak maximum at 115°C extending upwards from 90 to 120°C and a much sharper peak at 122°C, see Table 6. The T_g may be attributed to the random EP copolymer structure and both endotherms to a small crystalline homopolymer or blocky component, the $\Delta H_{melting}$ for this process being only 0.41 J g^{-1}. The DSC curves for the blends show two clear features, a T_g at about −25°C and a sharp endotherm having a maximum at 50°C. However, there was some evidence from the DSC trace obtained for the 20 pph blend that a second lower temperature T_g was present. Further low temperature examination of these blends below −50°C was outside our instrument's capabilities. The change of specific heat capacity (ΔC_p) values determined for these blends at the T_g was less than that obtained for the EP rubber fraction alone, which confirms that the T_g process is in a bitumen-rich phase that is diminished by the dissolution of the rubber. The endothermic peak at 50°C seen for the blends is absent from the trace for EP rubber itself. This feature may be attributed to a low molecular weight paraffinic component of the bitumen crystallising, though the enthalpy value of this feature decreased as the rubber content in the blends increased. Létoffé et al. [17,18] have characterised paraffinic 'waxy' components found in crude oils (from which bitumen originates) by several techniques including DSC, and observed endotherms between 40 and 50°C for C_{25}–C_{35} paraffins.

The variations in tan δ and loss modulus (E'') with composition for this rubber's blends with 100 pen. bitumen over the temperature range −100 to 200°C are shown in Fig. 12. The presence of two T_gs in these blends is revealed in the loss modulus plots, one from the EP rubber-rich phase about −38°C, the other from a bitumen-rich phase at −10°C with almost an "isobestic point" in between, at about −28°C. The peak due to the EP rubber-rich phase becomes more intense with increasing rubber content, whereas the peak associated with the bitumen-rich phase broadened and shifted to higher temperatures once the polymer content reached 30 pph. Two features were also observed in the tan δ plots, a peak at −30°C which becomes more resolved with increasing polymer content and a second process present as a shoulder at about 40°C close to the temperature where endotherms were displayed in the DSC traces of the blends. The EP rubber–bitumen blends do not behave like swollen rubbers at elevated temperatures as the storage modulus curves fall away and do not level off, Fig. 13. The higher temperature

Table 4
DSC characteristics of blends of bitumen with α-olefin copolymer, Vestoplast 891

pph Polymer	10	20	30	40	V.891
% Polymer	9.1	16.7	23.1	28.6	100
T_g (°C)	−40	−39	−39	−38	−31
T_m (°C)	152	153	154	153	160
ΔHT_m (J g^{-1})	0.78	1.65	1.87	2.11	7.97

Table 5
DSC characteristics of blends of bitumen with EP graft copolymer, Adflex

pph Polymer	10	20	30	40	Adflex
% Polymer	9.1	16.7	23.1	28.6	100
$T_{g(1)}$ (°C)	−43	−39	−38	−39	−37
$\Delta C_p T_{g(1)}$ (J g^{-1} deg^{-1})	0.02	0.038	0.049	0.042	0.17
$T_{g\,(2)}$ (°C)	−11	2	11	11	NA[a]
$\Delta C_p T_{g(2)}$ (J g^{-1} deg^{-1})	0.026	0.025	0.029	0.059	NA[a]
T_m (°C)	130	131	132	132.5	145
ΔHT_m (J g^{-1})	1.26	2.56	3.53	4.46	13.61

[a] Not applicable.

properties may in part be controlled by the crystalline paraffinic component of the bitumen, manifested by the shoulder process seen in the tan δ graphs and by a sharp endotherm in the DSC traces. However, the blends persisted within the measurement system some 20°C above the temperature at which the endotherm melted, perhaps reflecting a viscoelastic stiffening of the polymer which remains at these temperatures.

3.6. Activation energies E_a, from the tan δ values

Arrhenius activation energies (±10%) were obtained on the prominent relaxations at the glass transitions. The measurements were made at the following frequencies, 0.3, 1, 3, 5 and 10 Hz, a restricted range that precluded an examination in terms of the Williams–Landel–Ferry equation [10], and the approximate temperature of the tan δ maxima using the 40 pph blends. For the five blends, IPP: 1300 kJ mol^{-1} at 57°C, APP: 600 kJ mol^{-1} at 15°C, α-olefin copolymer: 180 kJ mol^{-1} at −15°C, EP graft copolymer: 200 kJ mol^{-1} at −18°C and for the EP rubber: 160 kJ mol^{-1} at −28°C. For the APP blend, the temperature corresponds to the T_g of the pure polymer [10], but here the polymer-rich phase is continuous. Clearly the activation energies fall with the temperatures of the process and approximately with the ΔH fusion of the pure polymer or of the 40 pph blend itself, as may be seen by consulting Tables 2–6. These E_a values are well above those found in dielectric studies on polymers isolated in solution, (10–40 kJ mol^{-1}) [10], but are similar to those found for a poly(ether ether ketone) studied in the bulk [19] over restricted ranges. The values found here reflect a property of the amorphous phase that is rich in mobile polymer chains, but which is subject to constraints from the crystalline phases as well as components of the bitumen.

4. Conclusions

Fluorescence microscopy found that each blend has regions which were polymer-rich and others that were bitumen-rich. Since the domains were of 2–50 μm in size, much larger than the dimensions of the polymers, and had shapes that derived from the mixing stress, these were true phases, rather than microphases. The extent of the polymer-rich phase indicated that it might contain components of the bitumen too, so that for example, for the APP material there was a phase inversion once the polymer concentration reached 30 pph.

DSC found melting endotherms for the blends at temperatures about 6–12°C below those of the pure materials, a depression that reflected the smaller size that the crystallites had when they formed on cooling within the blends. In certain cases the crystallite melting was accompanied by an onset of flow, suggesting that the crystallites then served to crosslink extended polymer chains to create a gel-like network [12]. With IPP at a concentration of 40 pph the modulus of the blend was so high at 150°C (about the same as for the bitumen itself at normal temperatures) that a very extensive lamellar morphology is postulated.

The modulus of the blends at ambient temperatures and below depended on the polymer, being 10^9 Pa for all the blends but those of the APP, which was considerably softer, with moduli of about 10^7 Pa similar to that of the bitumen itself. The softness was enhanced when the polymer fraction was 40 pph, for then the polymer-rich phase was extensive.

Table 6
DSC characteristics of blends of bitumen with the EP rubber

pph Polymer	10	20	30	40	EP rubber
% Polymer	9.1	16.7	23.1	28.6	100
T_g (°C)	−23	−21	−14	−11.5	−40
$\Delta C_p T_g$ (J g^{-1} deg^{-1})	0.063	0.068	0.052	0.025	0.041
T_m (°C)	55.5	54.5	48	47	55 & 122
ΔHT_m (J g^{-1})	5.69	3.09	1.50	1.21	0.41

Upon this phase inversion, the modulus fell to about 3×10^5 Pa, and at ambient temperatures a significant peak in the tan δ plot was then also apparent. A loss process developed clearly for the α-olefin copolymer blends at −20°C in the tan δ plot once the concentration was above 20 pph, as it did also—but less prominently—for the EP graft polymer's blends. The random EP rubber, in contrast, produced a loss process at a lower temperature, about −30°C. At 0°C a 10 pph portion of this rubber causes a significant hardening of the bitumen, but, in contrast to the IPP, extra additions then lead to progressive softening. The α-olefin copolymer is similarly effective, but the "atactic polypropylene" does not cause the hardening in low proportions and creates finally a softer blend. Such variations in E' at low temperatures reflect the manner in which the stiff asphaltene component responds to subtle prompts from the various polymers, as much as the polymer itself.

We can see that two properties of these blends relate to their possible use in built-up roofing systems: the onset of flow at high (torching) temperatures takes place when crystallites present melt and so cease to crosslink the strands of polymer into a network. The low temperature flexibility of the blends derives from loss processes within the polymers, which are transferred to the blends, and are particularly prominent when the polymer-rich phases become extensive.

Acknowledgements

We acknowledge the financial and technical support of Dussek–Campbell Ltd, APP Polymers Division. The authors would like to thank the manufactures for supplying the polymers. (Our examination of these materials does not constitute an endorsement of their commercial value.) We are also grateful to GM McNally for access to a DMTA instrument.

References

[1] Fawcett AH, McNally T, McNally GM, Andrews F, Clarke J. Polymer 1999;40(22):6337.
[2] Fawcett AH, Lor S-K. Polymer 1992;33:2003.
[3] Prasad JV. J Polym Sci, Polym Chem Ed 1992;30:2033.
[4] Chiu Tak Ki. MSc Thesis. The Queen's University of Belfast, 1984.
[5] Cozewith C, Ver Strate G. Macromolecules 1971;4:482.
[6] Boor J. Ziegler–Natta catalysis and polymerisations. New York: Academic Press, 1979.
[7] Read J. Chem Br 1998;34:8 p. 46.
[8] Yen TF. Asphaltic materials. Encyclopedia of polymer science & engineering 1990:1 Index vol.
[9] Ait-Kadi A, Brahimi B, Bousmina M. Polym Engng Sci 1996;36:12 p. 1724.
[10] Bailey RT, North AM, Pethrick RA. Motion in high polymers. Oxford: Clarendon Press, 1981.
[11] Hoffman JD, Miller RL. Polymer 1997;38:3151.
[12] Hauser G, Schmidtke J, Strobl G. Macromolecules 1998;31:6250.
[13] te Nijenhuis K. Adv Polym Sci 1997;130:1.
[14] Lieberman RB, Bare PC. Propylene polymers, Encyclopedia of polymer science & engineering, 13. Chichester: Wiley, 1990. p. 464.
[15] Elias H-G. Macromolecules, 1. London: Wiley, 1977.
[16] McNally T. PhD Thesis. The Queen's University of Belfast, 1996.
[17] Létoffé JM, Claudy P, Chagué B, Orrit J. Fuel 1988;67:58.
[18] Létoffé JM, Claudy P, Garcin M, Volle JL. Fuel 1995;74:1.
[19] Kalika DS, Krishnasuramy RK. Macromolecules 1993;26:4060.